RSC Advances

PAPER

View Article Online
View Journal | View Issue

Cite this: *RSC Adv.*, 2024, **14**, 11350

Fine-tuning of organic optical double-donor NLO chromophores with DA-supported functional groups†

Abdul Rahman, [abcd] Shuhui Bo,*[cd] Amjad Ali, [aeh] Lian Zhang,[f] Suliman Yousef Alomer[g] and Fenggang Liu *[f]

Received 3rd December 2023
Accepted 4th January 2024

DOI: 10.1039/d3ra08246f

rsc.li/rsc-advances

New strategic chromophores with updated fine-tuning of previously reported **BLD1** and **BLD3** chromophores were designed. **BLD1** and **BLD3** have silicon functional groups on the donor unit, and the bridge has a good chance of self-assembling, so in the present study we fine-tuned the isolating groups to the bulky cyclic alkene to improve their dipole moment and organic electro-optic (OEO) properties as well. To demonstrate the impact of cyclic alkenes on the electron-donating groups in sensible NLO chromophore designs, a thorough analysis and comparison of the chromophore synthesis, UV-Vis calculations, solvatochromic behavior of the chromophore, DFT quantum mechanical calculations, thermal stabilities, and much lower dipole moments was conducted.

Introduction

Organic electro-optic (OEO) materials have recently attracted significant interest because of the increased reliance on online work owing to the widespread impact of COVID-19. Organic electric-optic materials play a key role in moving forward with the next-generation network and 5G. Optical technology advancements are essential to improve our entire communication.[1] Most of our networks such as optical broadband and 5G are directly dependent on the performance and advancement of OEO materials.[2] An electro-optic modulator is a device that helps to upload electronic signals onto optical carriers, and an electro-optic module is the core component devised by using OEO materials.[3]

Nowadays, most commercially available devices are based on inorganic materials such as lithium niobite ($LiNbO_3$) and inorganic crystal materials.[4] However, OEO materials possess advantageous characteristics such as easy processing, fast response, speedy and good processability, low cost, and a larger electro-optic coefficient and have robust applications in high-speed information transmission, optical communication,[1] optical information storage,[5] and terahertz technology, surpassing commercially available inorganic materials.[4,6,7]

There are still many challenges that need to be solved in the synthesis of OEO materials, such as optimizing the structural features of OEO materials to obtain a larger electro-optic coefficient (r_{33}), and improving their photothermal as well as polarization orientation stability.[8] The non-centrosymmetric arrangement of OEO chromophores directly affects the electro-optic properties under an electric field. The anti-parallel packing of chromophores is directly proportional to the macroscopic electro-optic coefficient, and chromophores with high dipole moments and electrostatic interactions between the molecules can lead to a restriction of the anti-parallel packing of the chromophores.[9] Therefore, the designs of chromophores need to have weak electrostatic forces between the molecules in the polymer matrix, which would lead to a high electro-optic coefficient.[10] In general, the configuration of chromophores is divided into a few major components, such as the electron donor, π-bridge, and electron acceptor (D–π–A).[11] Many researchers are attempting to tackle these issues by modifying the chromophore through the insertion of bulky electron-rich donors, electron-deficient acceptors, and π bridges (Fig. 1).[12,33]

According to the literature, significant attention has been paid to the modification of the electron bridge and accepter to improve the performance of second-order nonlinear optical materials.[13] However, the electron donor, which has played a crucial role in the performance of EOE materials, has received

[a]*Department of Polymer Science and Engineering, Zhejiang University, Hangzhou 310027, China*
[b]*ZJU-Hangzhou Global Scientific and Technological Innovation Center, Hangzhou 311215, China*
[c]*Optoelectronics Research Centre, School of Science, Minzu University of China, Beijing, 100081, P. R. China. E-mail: boshuhui@muc.edu.cn*
[d]*Engineering Research Centre of Photonic Design Software, Ministry of Education, P. R. China*
[e]*School of Material Science & Engineering, Jiangsu University, Zhenjiang, 212013, P.R. China*
[f]*Guangzhou University, Guangzhou, 510006, P. R. China. E-mail: liufg6@gzhu.edu.cn*
[g]*Zoology Department, College of Science, King Saud University, Riyadh 11451, Kingdom of Saudi Arabia*
[h]*Institute of Chemistry University of Silesia, Szkolna 9, Katowice 40-600, Poland*

† Electronic supplementary information (ESI) available. See DOI: https://doi.org/10.1039/d3ra08246f

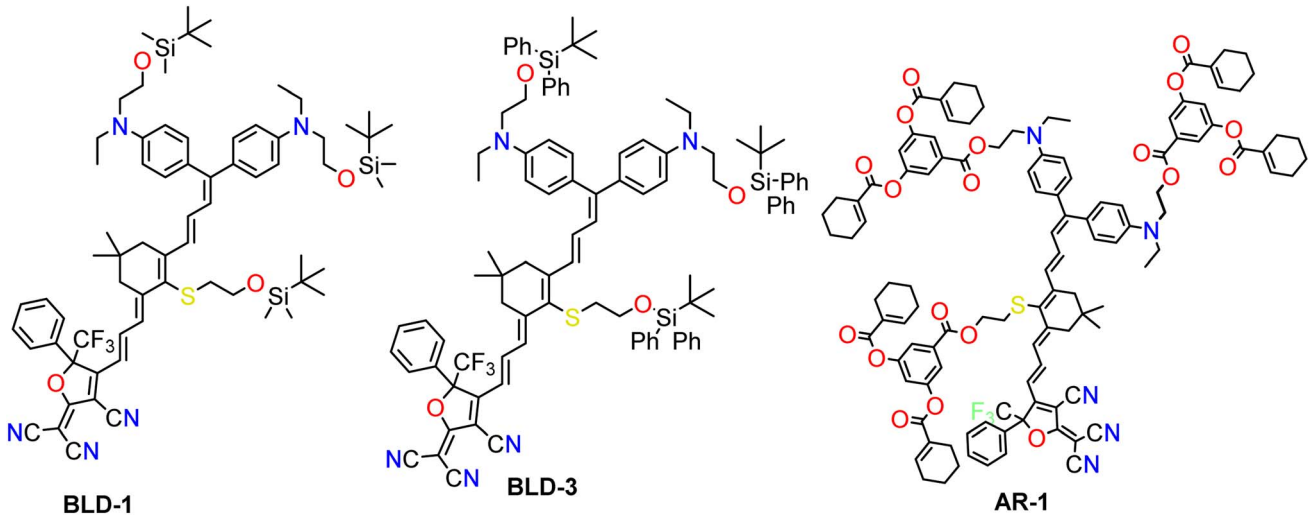

Fig. 1 Chemical structure of chromophores BLD-1, 3 and AR-1.

minimal attention.[14] Most of the reported donors belong amine-based derivatives, such as 4-(dialkylamino)phenyl groups,[15] triphenylamine,[16] and second-order nonlinear optical (NLO),[17] third-order NLO, two-photon absorption,[18] and hole-transport materials.[19] Previously, some research groups used DFT calculations to compare the systematic strength of different amine groups, yielding valuable insights for the design of excellent OEO materials.[20] Based on the results of DFT calculations, we designed a novel chromophore that possesses a strong electron-donating capability, an electron-rich bridge, and a strong electron-acceptor capability, as well as very bulky groups on the donor and bridge to avoid self-assembly (Fig. 2).[21,33]

This work involves the invention of a novel chromophore, which includes modifications to the previously published **BLD1** and **BLD3** chromophores developed by our research team. **BLD1** and **BLD3** have silicon functional groups on the donor and bridge, which increases the likelihood of self-assembly; therefore, we changed the silicon functional groups to a bulky cyclic alkene to improve the material's dipole moment and EOE properties.[22] The chromophore synthesis, UV-vis calculations, solvatochromic behavior of the chromophore, DFT quantum

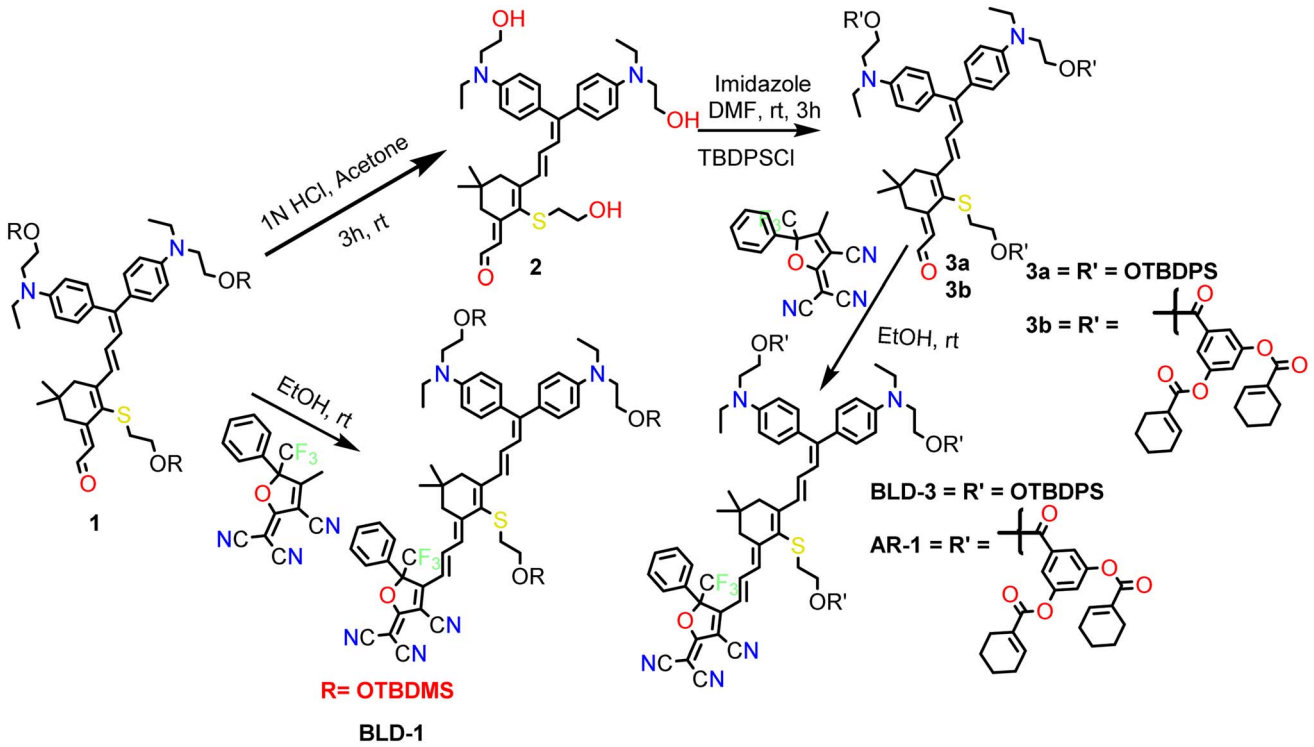

Fig. 2 Synthetic routes for chromophores BLD-1, 3 and AR-1.

mechanical calculations, thermal stabilities, and EO activities of the synthesized chromophores were systematically studied and compared to illustrate the influence of electron-donating groups on rational NLO chromophore design.

Thermal stability

Thermal stability is the basic requirement for the poling process and EO device application; therefore, chromophores must show stability over 150 °C temperature.[23] The thermal stability of the synthesized chromophore was investigated using thermogravimetric analysis (TGA) under nitrogen at a heating rate of 10 °C per min and the results are plotted in the graph in Fig. 3. The decomposition temperatures (T_d, 5% weight loss) of all the synthesized chromophores were found to be above 200 °C, which is a clear indication that these chromophores were well suited for making an EO device and for exploring the applications of the poling process. From all three synthesized chromophores, the chromophore **AR-1** exhibited the highest decomposition temperature (T_d, 285 °C) among all the synthesized chromophores, such as **BLD3** (T_d, 225 °C) and chromophore **BLD1** (T_d, 207 °C). The differences in decomposition temperature between these chromophores could be attributed to the different kinds and sizes of isolation groups in each chromophore, and as the **AR-1** chromophore exhibited the highest decomposition temperature because of its bulky and strong bonding functional groups. Therefore, the exceptional thermal stabilities of the newly designed chromophore render them highly suitable and compatible for practical device fabrication and the development of EO devices (Fig. 4).

Optical properties

The UV-visible absorption spectra of the three synthesized chromophores in different solvents, from low to high polarity, with different dielectric constants. Were investigated to observe

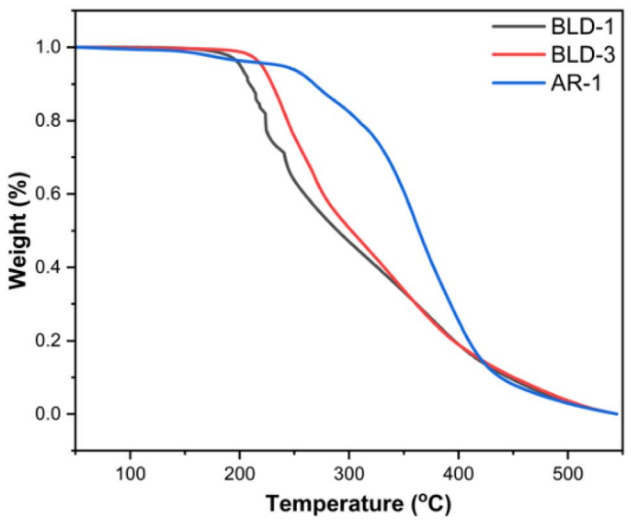

Fig. 3 TGA curves of **BLD-1**, **3** and **AR-1** obtained at a heating rate of 10 °C min^{-1} in a nitrogen atmosphere.

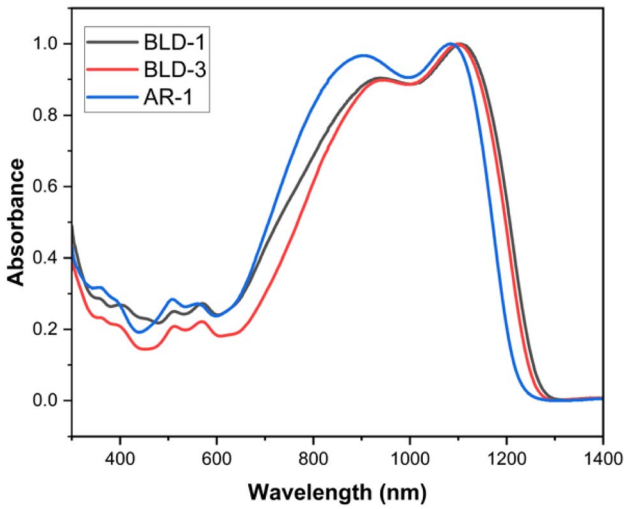

Fig. 4 UV-Vis absorption spectra of the chromophores **BLD-1**, **3** and **AR-1** in films.

the effects of different kinds of isolation groups on the charge-transfer absorption properties, as shown in Fig. 5; and the observed spectrum data are summarized in Table 2. The synthesized chromophores **BLD-1**, **BLD-3**, and **AR-1** exhibited absorption maxima (λ_{max}) in chloroform at 891, 905, and 857 nm, respectively. The remarkable differences in absorption maxima provide compelling evidence that changing the isolation groups has a strong effect on the charge-transfer properties of the chromophores.[24] These findings suggest that the neutral form of chromophores in the ground state will prevail over the charged separated form.[25] The absorption maxima (λ_{max}) values of **AR-1** were hypsochromically shifted to (*ca.* 34–48 nm) compared to those of the corresponding analogs **BLD-1** and **BLD-3**, which was probably due to the introduction of the new donor having an electron-accepting ester group. These donors have lower electron-donating capability, but they have the functional group necessary for the DA reaction, enabling their transformation into large dendrimers exhibiting supramolecular characteristics. The significant differences in the absorption spectra were due to the different electronic properties and bulkiness of the isolation group. The chromophores **BLD-1** and **BLD-3** had the same kinds of different isolation groups, TBDMS and TBDPS, respectively. However, the chromophore having a more steric isolating group (TBDPS) was bathochromically shifted (*ca.* 13–14 nm) compared to the chromophore having a less steric isolation group (TBDMS); however, in the case of the chromophore **AR-1**, which has an electron-withdrawing ester group and more steric isolation groups than **BLD-1** and **BLD-3**, it displayed a hypsochromic shift (*ca.* 85–103 nm).

In addition, the solvatochromic behavior of the synthesized chromophores in different solvents with different polarities was examined.[26] A broad π–π* intramolecular charge-transfer (ICT) absorption band was found in all chromophores. The synthesized chromophores had remarkable distinct optical features in the solvatochromic and absorption bands in polar solvents, such as chloroform and acetonitrile. All the chromophores

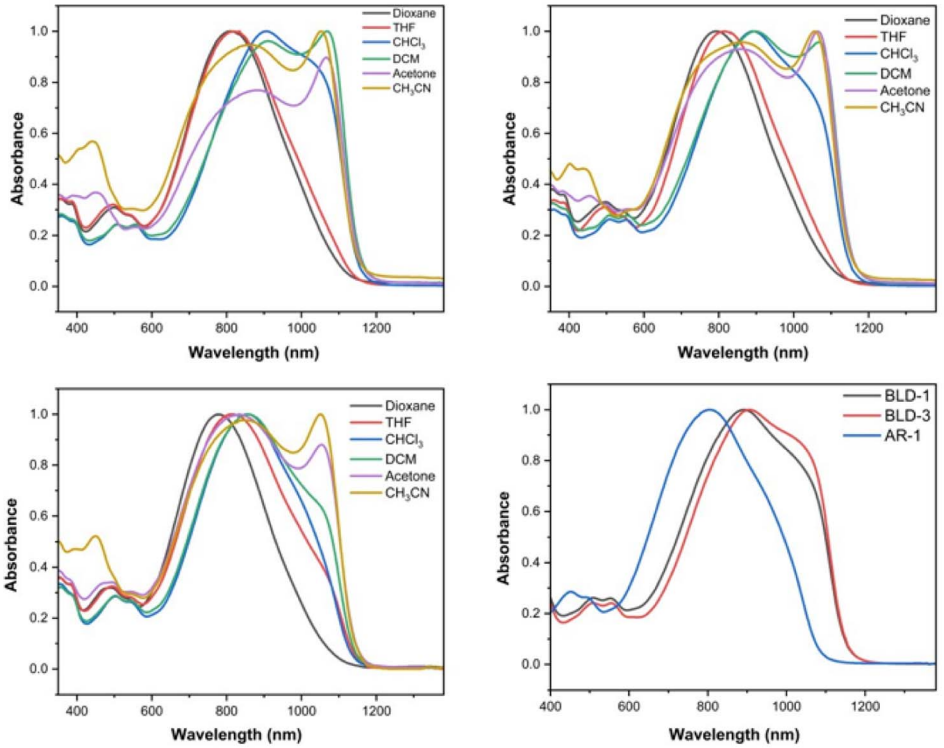

Fig. 5 UV-Vis absorption spectra of the chromophores **BLD-1**, **3** and **AR-1** in six kinds of aprotic solutions with different varying dielectric constants and the chromophores **BLD-1**, **3** and **AR-1** in chloroform.

continuously shifted from smaller to longer wavelengths when the solvent polarity was shifted from low polar to high polar solvents such as dioxane to chloroform. However, this followed a reverse order for the absorption maxima (hypsochromic) when the polarity of solvents was shifted for more highly polar solvents, such as from chloroform to acetonitrile. The absorption maxima of all chromophores were also investigated in the film. The film absorption maxima of **BLD-1**, **BLD-3**, and **AR-1** were 1105, 1099, and 1093 nm, respectively, which were totally different from the absorption maxima in solutions. This difference may be due to several mechanisms, such as the self-assembly and strong interactions between chromophores in the solid state.[27]

Theoretical calculations

The ground state polarization and microscopic NLO properties of all the synthesized chromophores were deeply investigated, and the effect of different isolation groups on these properties was studied using DFT calculations in the Gaussian 09 program package at the CAMB3LYP level by employing the split valence 6-31g(d) basis set.[28] In all the DFT calculations, such as the first hyperpolarizability (β), dipole moments (μ), and HOMO–LUMO energy gaps, all the chromophores were supposed to be in the *trans* state, and the results are summarized in Table 1 and Fig. 6.[29]

The HOMO–LUMO energy gap is crucial for determining the capacity of the charge-transfer interaction between the chromophores. We performed DFT calculations on all chromophores to determine the HOMO–LUMO energy gaps. The calculated values for the energy gaps were 1.73, 1.75, and 1.79 eV, respectively. The energy gap between the highest occupied molecular orbital (HOMO) and the lowest unoccupied

Table 1 Thermal and optical properties data of the chromophores

Compounds	λ_{max} [nm]	ΔE(DFT)[a] (eV)	β_{tot}[b] (10^{-30} esu)	μ[c] (D)
BLD1	891	1.746	1722	27.79
BLD3	905	1.750	1732	28.58
AR-1	802	1.799	1353	20.97
JRD1[d]	784	1.94	1030	26.19
YLD124[d]	786	2.057	464	22.35

[a] Calculated from DFT calculations. [b] First-order hyperpolarizability calculated from DFT calculations. [c] Total dipole moment. [d] See ref. 21.

Table 2 Thermodynamic and UV absorption data of the chromophores

Compound	T_d (°C)	λ_{max}[a]	λ_{max}[b]	$\Delta\lambda$[c]	λ_{max}[d]
BLD1	207	891	789	102	1105
BLD3	225	905	807	98	1099
AR-1	285	857	781	76	1087

[a] (nm) measured in chloroform. [b] (nm) measured in dioxane. [c] (nm) difference between λ_{max} and λ_{max}. [d] (nm) measured in film, respectively.

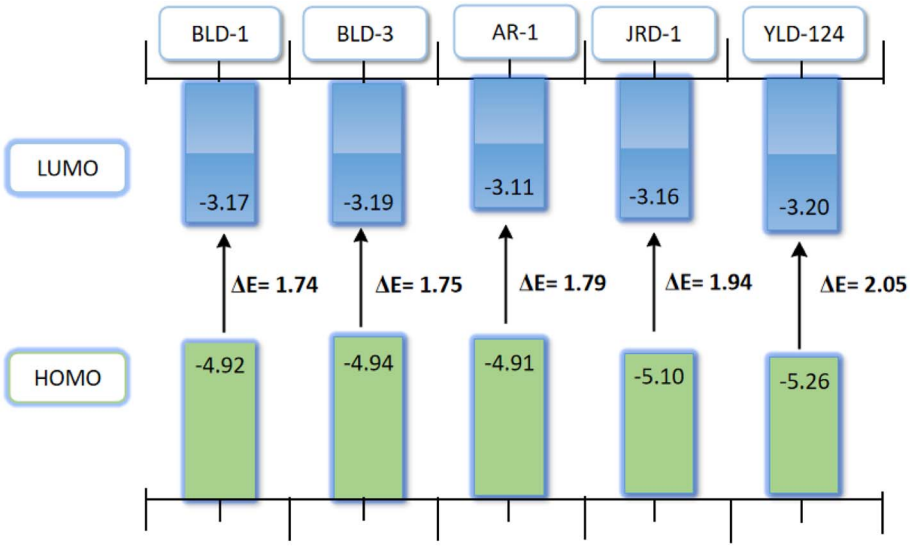

Fig. 6 HOMO and LUMO energy levels of the chromophores.

molecular orbital (LUMO) thus increased in the series of chromophores. This indicates that the ability of charge transfer within the molecules was limited or hindered. Consequently, the chromophore with a larger HOMO–LUMO energy gap exhibited smaller values for the absorption maxima (λ_{max}). The inferences drawn from the DFT calculations aligned closely with the findings obtained from the UV-vis spectroscopic research.

The HOMO–LUMO energy gap impacts the β value of chromophores, exhibiting an inverse relationship; whereby when the gap increased, the β value decreased and *vice versa*.[30] The β value of chromophores plays a crucial role in the optical properties of chromophores. The chromophores **BLD-1** and **BLD-3** had lower energy gaps than the chromophore **AR-1**. This indicates that the first two chromophores have a greater likelihood of electron localization and a significant first-order hyperpolarizability β value compared with the chromophore **AR-1**. The calculated first-order hyperpolarizability of **AR-1** was 1353 because of electron withdrawal and the presence of a bulky steric isolating group on the chromophore, but the dipole moment of **AR-1** was less than that of **BLD-1** and **BLD-3**. The dipole moment also plays a key role in the manufacturing of EO devices, and a chromophore with a smaller dipole moment is an excellent choice for manufacturing EO devices.[31] We also calculated the first-order hyperpolarizabilities of the classical chromophores **JRD1** and **YLD124**, and compared the values with those of the synthesized chromophores. The first-order hyperpolarizability of chromophore **AR-1** was 1.31 times higher than that of **JRD1** and 2.91 times higher than that of **YLD124**. The differences in values were due to the narrow gap of the HOMO–LUMO of the **AR-1** chromophore as compared to **JRD1** and **YLD124**.

The smaller energy gaps and higher first-order hyperpolarizabilities of **BLD-1** and **BLD-3** could be attributed to the isolating group. Unlike **AR-1**, which has an ester group that withdraws electron density, **BLD-1** and **BLD-3** do not have this electron-withdrawing functionality. The **AR-1** chromophore was preferred over **JRD1** and **YLD124** only because of the introduction of a double electron-donor isolating group, which is a more powerful donor and allows for easier charge separation compared to the single electron donors in **JRD1** and **YLD124**.[32] The β values determine the influence of donor groups on the absorption charge-transfer band. The trend of increasing λ_{max} was consistent with the increasing β value, as shown in Fig. 5.

Materials and instruments

All chemicals were commercially purchased and used without further purification unless otherwise stated. Ultra-dry reagent solvents, such as *N*,*N*-dimethyl formamide (DMF) and tetrahydrofuran (THF), were purchased from reagent companies. Precoated analyses of 0.25 mm thick TLC silica plates were performed, and spots were visualized under UV light. Kieselgel (200–300 mesh) of silica gel was used for the silica gel chromatography. ^{1}H NMR spectra were recorded on an Advance Bruker 500M (500 MHz) NMR spectrometer (with tetramethylsilane as an internal reference). The MS spectra were obtained by matrix-assisted laser desorption/ionization of flight (MALDI-TOF) on a BIFLEXIII (Broker Inc.) spectrometer. The UV-vis spectra were recorded on a Shimadzu UV-1800 photospectrometer. TGA was performed using a PerkinElmer TGA-4000 system at a heating rate of 10 °C min^{-1} under nitrogen protection.

Beside **3b**, all the procedures have been already reported in the literature.[33]

Synthesis of 3b

3,5-Bis((cyclohex-1-ene-1-carbonyl)oxy)benzoic acid (0.50 g, 0.082 mmol), *N*,*N*-dimethylpyridin-4-amine (0.010 g, 0.0082 mmol), and EDCl (1.36 g, 0.0082 mmol) were added to a Schlenk tube and purged with N_2. Next, 30 mL of dry DCM was added to the reaction flask, which was then cooled at 0 °C. A solution of

(*E*)-2-(3-((*E*)-4,4-bis(4-(ethyl(2-hydroxyethyl)amino)phenyl)buta-1,3-dien-1-yl)-2-((2-hydroxyethyl)thio)-5,5-dimethylcyclohex-2-en-1-ylidene)acetaldehyde compound **2** (0.5 g, 0.827 mmol) in 10 mL DCM was slowly added to the above solution. The reaction was kept for 3 h at 0 °C, and then the reaction mixture was shifted to room temperature. After completion of the reaction based on TLC, the reaction was quenched by adding 100 mL of water. The organic phase was extracted with ethyl acetate, washed with brine, and dried over $MgSO_4$. After removing the solvent in a vacuum, the crude product was purified by silica chromatography and eluted with ethyl acetate/hexane (1 : 15 to 1 : 10) to give compound **3b** as an oil in a 90% yield (0.98 g, 0.59 mmol). MS (MALDI) (M+, $C_{99}H_{108}N_2O_{19}S$): calcd: 1661.73; found: 1661.70. ^{1}H NMR (600 MHz, chloroform-d) δ 10.14 (d, J = 8.0 Hz, 0H), 7.70 (d, J = 2.2 Hz, 1H), 7.68 (d, J = 2.2 Hz, 1H), 7.61 (d, J = 15.2 Hz, 0H), 7.26 (dtt, J = 11.5, 3.8, 1.7 Hz, 1H), 7.22 (ddt, J = 5.7, 4.5, 2.0 Hz, 1H), 7.20–7.12 (m, 2H), 6.98 (d, J = 8.0 Hz, 0H), 6.90 (dd, J = 15.2, 11.2 Hz, 0H), 6.83–6.80 (m, 1H), 6.71–6.60 (m, 1H), 4.53 (t, J = 6.5 Hz, 1H), 4.49 (t, J = 6.6 Hz, 1H), 4.36 (t, J = 6.9 Hz, 1H), 3.77 (t, J = 6.5 Hz, 1H), 3.71 (t, J = 6.6 Hz, 1H), 3.53 (q, J = 7.0 Hz, 1H), 3.48 (q, J = 7.0 Hz, 1H), 2.94 (t, J = 6.9 Hz, 1H), 2.42–2.21 (m, 9H), 1.82–1.61 (m, 9H), 1.27 (td, J = 7.1, 3.4 Hz, 2H), 1.21 (t, J = 7.1 Hz, 1H). ^{13}C NMR (151 MHz, $CDCl_3$) δ 191.50, 165.31, 165.23, 165.14, 165.04, 164.75, 156.26, 151.52, 151.50, 151.42, 147.91, 147.50, 147.28, 142.98, 142.93, 142.80, 135.48, 132.31, 131.80, 131.27, 130.50, 129.84, 129.45, 129.44, 129.39, 127.43, 127.00, 126.78, 124.29, 120.72, 120.63, 120.24, 120.20, 120.13, 111.34, 111.22, 63.75, 62.70, 62.44, 60.41, 48.73, 48.68, 45.52, 45.40, 41.52, 39.94, 33.09, 30.03, 28.22, 26.10, 26.07, 24.16, 24.14, 21.98, 21.97, 21.32, 21.30, 21.06, 14.21, 12.44.

Synthesis of the chromophore AR-1

Compound **3b** (0.5 g, 0.52 mmol) and 2-(3-cyano-4-methyl-5-phenyl-5-(trifluoro-methyl)furan-2(5*H*) ylidene)malononitrile (0.18 g, 0.58 mmol) in anhydrous ethanol (10 mL) were added to a two-necked flask in a nitrogen atmosphere. After reacting for 6 h at 65 °C, the solution was concentrated using a rotary evaporator. The crude product was purified by column chromatography using ethyl acetate and hexane (v/v, 1 : 8 to 1 : 1) as the eluent to give chromophore **AR-1** as a green solid in an 80% yield (0.52 g, 0.42 mmol). HRMS (ESI) (M+, $C_{115}H_{114}F_3N_5O_{19}S$): calcd: 1958.78; found: 1958.58. ^{1}H NMR (600 MHz, chloroform-d) δ 7.96 (s, 1H), 7.73–7.61 (m, 7H), 7.58–7.48 (m, 5H), 7.42 (d, J = 12.4 Hz, 1H), 7.28–7.20 (m, 10H), 7.19–7.12 (m, 3H), 6.82 (d, J = 8.3 Hz, 2H), 6.71 (dd, J = 22.8, 10.0 Hz, 3H), 6.42 (d, J = 14.4 Hz, 1H), 4.53 (t, J = 6.6 Hz, 2H), 4.49 (t, J = 6.5 Hz, 2H), 4.33 (td, J = 6.7, 1.9 Hz, 2H), 3.78 (t, J = 6.5 Hz, 2H), 3.73 (t, J = 6.6 Hz, 2H), 3.52 (dq, J = 28.0, 7.0 Hz, 4H), 2.94 (t, J = 6.6 Hz, 2H), 2.39–2.33 (m, 15H), 2.28 (dt, J = 7.3, 3.3 Hz, 12H), 1.76–1.70 (m, 12H), 1.69–1.60 (m, 10H), 1.28 (t, J = 7.1 Hz, 8H), 1.23 (t, J = 7.0 Hz, 3H). ^{13}C NMR (151 MHz, $CDCl_3$) δ 175.83, 171.19, 165.31, 165.22, 165.13, 165.04, 164.70, 162.17, 157.71, 155.18, 151.72, 151.54, 151.48, 148.21, 147.86, 147.02, 143.02, 142.97, 139.48, 132.74, 131.72, 131.59, 131.49, 131.23, 130.60, 130.23, 130.03, 129.61, 129.43, 129.40, 129.14, 128.45, 127.01, 126.81, 125.54, 124.87, 120.86, 120.76, 120.23, 120.11, 116.94, 111.66, 111.54, 111.37, 111.18, 111.00, 63.44, 62.54, 62.30, 60.41, 48.72, 48.66, 45.59, 45.46, 41.62, 41.16, 34.03, 30.32, 28.50, 27.73, 26.10, 24.15, 21.97, 21.30, 21.06, 14.21, 12.43.

Conclusion

We developed a new bulky chromophore with extremely low dipole moments and very high β values compared to conventional **JRD1** and **YLD124** chromophores by modification of the previously reported **BLD1** and **BLD3** chromophores developed by our research team. **BLD1** and **BLD3** possess silicon-based isolating groups on the donor and bridge, which increases the likelihood of self-assembly. Therefore, we replaced the silicon functional groups with a bulky cyclic alkene to improve their dipole moment and β values compared to conventional chromophores. This study involved several steps, including the synthesis of the chromophore, UV–vis calculations, analysis of the solvatochromic behavior, DFT quantum mechanical calculations, and evaluation of the thermal stabilities. The synthesized chromophores were systematically studied and compared to illustrate the influence of the cyclic alkene on electron-donating groups on rational NLO chromophore design.

Author contributions

Conceptualization and methodology: Abdul Rahman, Fenggang Liu, and Shuhui Bo. Data collection and analysis was performed by Amjid Ali and Lian Zhang. Writing review and editing: Suliman Yousef Alomer. All the authors read and agreed the final manuscript. Fenggang Liu and Shuhui Bo are the corresponding authors.

Conflicts of interest

There are no conflicts to declare.

Acknowledgements

This work was supported by the Guangzhou Municipal Science and Technology Project (No. 202102010426), the National Natural Science Foundation of China (No. 21805049), and the Scientific Research Projects (YBN2020085) of Huawei Technologies Co., Ltd. Fenggang Liu would like to thank Dr Chungai Hui at Huawei Technologies Co., Ltd and Hui Chen at the State Key Laboratory of Optoelectronic Materials and Technology (Sun Yat Sen University) for their invaluable discussions and help in this work. The authors would also like to thank the Researchers Supporting Project Number (RSP2024R35) King Saud University, Riyadh Saudi Arabi.

References

1 M. Burla, C. Hoessbacher, W. Heni, C. Haffner, Y. Fedoryshyn, D. Werner, T. Watanabe, H. Massler, D. L. Elder, L. R. Dalton and J. Leuthold, 500 GHz

plasmonic Mach-Zehnder modulator enabling sub-THz microwave photonics, *APL Photonics*, 2019, **4**(5), 056106.

2 Y. A. Getmanenko, T. G. Allen, H. Kim, J. M. Hales, B. Sandhu, M. S. Fonari, K. Y. Suponitsky, Y. Zhang, V. N. Khrustalev, J. D. Matichak, T. V. Timofeeva, S. Barlow, S.-H. Chi, J. W. Perry and S. R. Marder, Linear and Third-Order Nonlinear Optical Properties of Chalcogenopyrylium-Terminated Heptamethine Dyes with Rigid, Bulky Substituents, *Adv. Funct. Mater.*, 2018, **28**(46), 1804073.

3 U. Koch, C. Uhl, H. Hettrich, Y. Fedoryshyn, C. Hoessbacher, W. Heni, B. Baeuerle, B. I. Bitachon, A. Josten, M. Ayata, H. Xu, D. L. Elder, L. R. Dalton, E. Mentovich, P. Bakopoulos, S. Lischke, A. Krüger, L. Zimmermann, D. Tsiokos, N. Pleros, M. Möller and J. Leuthold, A monolithic bipolar CMOS electronic–plasmonic high-speed transmitter, *Nat. Electron.*, 2020, **3**(6), 338–345.

4 L. R. Dalton, D. Lao, B. C. Olbricht, S. Benight, D. H. Bale, J. A. Davies, T. Ewy, S. R. Hammond and P. A. Sullivan, Theory-inspired development of new nonlinear optical materials and their integration into silicon photonic circuits and devices, *Opt. Mater.*, 2010, **32**(6), 658–668.

5 C. Haffner, A. Joerg, M. Doderer, F. Mayor, D. Chelladurai, Y. Fedoryshyn, C. I. Roman, M. Mazur, M. Burla, H. J. Lezec, V. A. Aksyuk and J. Leuthold, Nano–opto-electro-mechanical switches operated at CMOS-level voltages, *Science*, 2019, **366**(6467), 860–864.

6 Y. Salamin, I.-C. Benea-Chelmus, Y. Fedoryshyn, W. Heni, D. L. Elder, L. R. Dalton, J. Faist and J. Leuthold, Compact and ultra-efficient broadband plasmonic terahertz field detector, *Nat. Commun.*, 2019, **10**(1), 5550.

7 J.-A. Lee, W. T. Kim, M. Jazbinsek, D. Kim, S.-H. Lee, I. C. Yu, W. Yoon, H. Yun, F. Rotermund and O.-P. Kwon, X-Shaped Alignment of Chromophores: Potential Alternative for Efficient Organic Terahertz Generators, *Adv. Opt. Mater.*, 2020, **8**(9), 1901921.

8 M. Jin, Z.-C. Zhu, Q.-Y. Liao, Q.-Q. Li and Z. Li, Dendronized Polymers with High FTC-chromophore Loading Density: Large Second-order Nonlinear Optical Effects, Good Temporal and Thermal Stability, *Chin. J. Polym. Sci.*, 2020, **38**(2), 118–125.

9 H. Xu, D. L. Elder, L. E. Johnson, Y. de Coene, S. R. Hammond, W. Vander Ghinst, K. Clays, L. R. Dalton and B. H. Robinson, Electro-Optic Activity in Excess of 1000 pm V−1 Achieved via Theory-Guided Organic Chromophore Design, *Adv. Mater.*, 2021, **33**(45), 2104174.

10 X. Zang, H. Liu, Q. Li, Z. a. Li and Z. Li, A TCBD-based AB2-type second-order nonlinear optical hyperbranched polymer prepared by a facile click-type postfunctionalization, *Polym. Chem.*, 2020, **11**(34), 5493–5499.

11 J. Wu, C. Peng, H. Xiao, S. Bo, L. Qiu, Z. Zhen and X. Liu, Donor modification of nonlinear optical chromophores: Synthesis, characterization, and fine-tuning of chromophores' mobility and steric hindrance to achieve ultra large electro-optic coefficients in guest–host electro-optic materials, *Dyes Pigm.*, 2014, **104**, 15–23.

12 F. Liu, S. Mo, Z. Zhai, M. Peng, S. Wu, C. Li, C. Yu and J. Liu, Synthesis of nonlinear optical chromophores with isophorone-derived bridges for enhanced thermal stability and electro-optic activity, *J. Mater. Chem. C*, 2020, **8**(27), 9226–9235.

13 D. Briers, L. De Cremer, G. Koeckelberghs, S. Foerier, T. Verbiest and C. Samyn, Influence of the Position of the Connecting Spacer of the Chromophore on the Nonlinear Optical Response, *Macromol. Rapid Commun.*, 2007, **28**(8), 942–947.

14 F. Liu, Z. Zeng, A. Rahman, X. Chen, Z. Liang, X. Huang, S. Zhang, H. Xu and J. Wang, Design and synthesis of organic optical nonlinear multichromophore dendrimers based on double-donor structures, *Mater. Chem. Front.*, 2021, **5**(24), 8341–8351.

15 Y.-J. Cheng, J. Luo, S. Hau, D. H. Bale, T.-D. Kim, Z. Shi, D. B. Lao, N. M. Tucker, Y. Tian, L. R. Dalton, P. J. Reid and A. K. Y. Jen, Large Electro-optic Activity and Enhanced Thermal Stability from Diarylaminophenyl-Containing High-β Nonlinear Optical Chromophores, *Chem. Mater.*, 2007, **19**(5), 1154–1163.

16 M. Yang, M. Peng, Z. Li, Z. Wang, F. Liu, W. Liu, J. Liao, T. Luo and J. Wang, Design and synthesis of Phenylaminothiophene donor-based chromophore with enhanced electro-optic activity, *Dyes Pigm.*, 2021, **192**, 109423.

17 H. Yang, Z. Cheng, C. Liu, W. Wu, K.-N. Zhang, S. Xu, Y. Liu, S. Cao and Z. Li, A second-order nonlinear optical dendronized hyperbranched polymer containing isolation chromophores: achieving good optical nonlinearity and stability simultaneously, *Sci. China: Chem.*, 2018, **61**(5), 584–591.

18 H. Ma, S. Liu, J. Luo, S. Suresh, L. Liu, S. H. Kang, M. Haller, T. Sassa, L. R. Dalton and A. K.-Y. Jen, Highly Efficient and Thermally Stable Electro-Optical Dendrimers for Photonics, *Adv. Funct. Mater.*, 2002, **12**(9), 565–574.

19 J. Zou, D. Zhang, W. Chen and J. Luo, Optimizing the vectorial component of first hyperpolarizabilities of push–pull chromophores to boost the electro-optic activities of poled polymers over broad telecom wavelength bands, *Mater. Adv.*, 2021, **2**(7), 2318–2327.

20 O. Kwon, S. Barlow, S. A. Odom, L. Beverina, N. J. Thompson, E. Zojer, J.-L. Brédas and S. R. Marder, Aromatic Amines: A Comparison of Electron-Donor Strengths, *J. Phys. Chem. A*, 2005, **109**(41), 9346–9352.

21 H. Xu, J. Liu, J. Liu, C. Yu, Z. Zhai, G. Qin and F. Liu, Self-assembled binary multichromophore dendrimers with enhanced electro-optic coefficients and alignment stability, *Mater. Chem. Front.*, 2020, **4**(1), 168–175.

22 Z. a. Li, P. Chen, Y. Xie, Z. Li and J. Qin, Ar–ArF Self-Assembly of Star-Shaped Second-Order Nonlinear Optical Chromophores Achieving Large Macroscopic Nonlinearities, *Adv. Electron. Mater.*, 2017, **3**(11), 1700138.

23 F. Liu, S. Chen, S. Mo, G. Qin, C. Yu, W. Zhang, W.-J. Shi, P. Chen, H. Xu and M. Fu, Synthesis of novel nonlinear optical chromophores with enhanced electro-optic activity

by introducing suitable isolation groups into the donor and bridge, *J. Mater. Chem. C*, 2019, **7**(26), 8019–8028.

24 Y.-J. Cheng, J. Luo, S. Huang, X. Zhou, Z. Shi, T.-D. Kim, D. H. Bale, S. Takahashi, A. Yick, B. M. Polishak, S.-H. Jang, L. R. Dalton, P. J. Reid, W. H. Steier and A. K. Y. Jen, Donor–Acceptor Thiolated Polyenic Chromophores Exhibiting Large Optical Nonlinearity and Excellent Photostability, *Chem. Mater.*, 2008, **20**(15), 5047–5054.

25 J. A. Davies, A. Elangovan, P. A. Sullivan, B. C. Olbricht, D. H. Bale, T. R. Ewy, C. M. Isborn, B. E. Eichinger, B. H. Robinson, P. J. Reid, X. Li and L. R. Dalton, Rational Enhancement of Second-Order Nonlinearity: Bis-(4-methoxyphenyl)hetero-aryl-amino Donor-Based Chromophores: Design, Synthesis, and Electrooptic Activity, *J. Am. Chem. Soc.*, 2008, **130**(32), 10565–10575.

26 W. Jin, P. V. Johnston, D. L. Elder, K. T. Manner, K. E. Garrett, W. Kaminsky, R. Xu, B. H. Robinson and L. R. Dalton, Structure–function relationship exploration for enhanced thermal stability and electro-optic activity in monolithic organic NLO chromophores, *J. Mater. Chem. C*, 2016, **4**(15), 3119–3124.

27 X.-H. Zhou, J. Luo, J. A. Davies, S. Huang and A. K. Y. Jen, Push–pull tetraene chromophores derived from dialkylaminophenyl, tetrahydroquinolinyl and julolidinyl moieties: optimization of second-order optical nonlinearity by fine-tuning the strength of electron-donating groups, *J. Mater. Chem.*, 2012, **22**(32), 16390–16398.

28 D. Zhang, W. Chen, J. Zou and J. Luo, Critical Role of Non-classical Intermolecular Hydrogen Bonding in Affecting the π–π Stacking and Nonlinear Optical Properties of Tricyanofuran-Based Push–Pull Heptamethines, *Chem. Mater.*, 2021, **33**(10), 3702–3711.

29 D. Zhang, J. Zou, W. Wang, Q. Yu, G. Deng, J. Wu, Z.-A. Li and J. Luo, Systematic study of the structure-property relationship of a series of near-infrared absorbing push-pull heptamethine chromophores for electro-optics, *Sci. China: Chem.*, 2021, **64**(2), 263–273.

30 J. Luo, F. Lin, Z. a. Li, M. Li, T.-D. Kim, S.-H. Jang and A. K. Y. Jen, New push–pull polyene chromophores containing a Michler's base donor and a tricyanofuran acceptor: multicomponent condensation, allopolar isomerism and large optical nonlinearity, *J. Mater. Chem. C*, 2017, **5**(9), 2230–2234.

31 H. Zhang, Y. Yang, H. Xiao, F. Liu, F. Huo, L. Chen, Z. Chen, S. Bo, L. Qiu and Z. Zhen, Enhancement of electro-optic properties of bis(N,N-diethyl)aniline based second order nonlinear chromophores by introducing a stronger electron acceptor and modifying the π-bridge, *J. Mater. Chem. C*, 2017, **5**(27), 6704–6712.

32 T.-D. Kim, J. Luo, Y.-J. Cheng, Z. Shi, S. Hau, S.-H. Jang, X.-H. Zhou, Y. Tian, B. Polishak, S. Huang, H. Ma, L. R. Dalton and A. K. Y. Jen, Binary Chromophore Systems in Nonlinear Optical Dendrimers and Polymers for Large Electrooptic Activities, *J. Phys. Chem. C*, 2008, **112**(21), 8091–8098.

33 Q. Zeng, X. Chen, A. Rahman, Z. Zeng, Z. Liang, L. Shi, Z. Huang, S. Bo, F. Liu and J. Wang, A modifiable double donor based on bis(N-ethyl-N-hydroxyethyl)aniline for organic optical nonlinear chromophores, *Mater. Chem. Front.*, 2022, **6**(8), 1079–1090.